Real-Time Fatigue Crack Growth Rate Estimation Methodology for Structural Health Monitoring of Ships

Article *in* IEEE Sensors Journal · October 2022

DOI: 10.1109/JSEN.2022.3204146

Prasannata Shivdas Bhange
Indian Institute of Technology Hyderabad

Deepak Kumar Joshi
Indian Institute of Technology Hyderabad

Sunil Kumar
University of Hyderabad

Kamal Mankari
University of Hyderabad

Real-time Fatigue Crack Growth Rate Estimation Methodology for Structural Health monitoring of Ships

Prasannata Bhange, Deepak Kumar Joshi, Sunil Kumar Pandu, Kamal Mankari, Swati Ghosh Acharyya, K. Sridhar and Amit Acharyya, *Member, IEEE*

***Abstract*—Fatigue experimental setups for studying the crack growth propagation in a high strength low alloy DMR 249A ship steel were arranged by loading the specimen with the real sea state conditions value of 4 for the application of structural health monitoring of ships. The experimental setup consists of a fatigue loading machine, acoustic emission (AE) sensors, AE nodes for pre-processing of data. In this investigation, a methodology to identify the crack propagation phenomenon in a specimen independent of the AE parameters has been developed. This methodology proves beneficial in identifying the noise and crack information in ship steel by creating the phase portraits of the time domain signal and indicating the same onto the phase portraits. A polynomial regression-based model for estimating the crack growth rate in the material has been developed by introducing a new parameter mean of box count (MBC).**

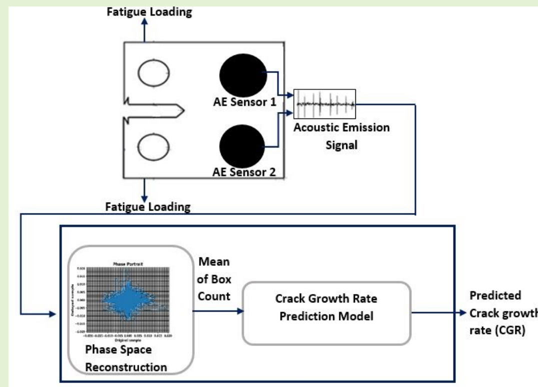

***Index Terms*—Acoustic emission (AE), phase space reconstruction (PSR).**

I. Introduction

SHIPS have been an important and common means of transport for goods and people for a very long period. They have been used in various sectors like military, commercial, and defence. Majorly all the ships are fabricated of steel. Over the years the ship's steel undergoes damage which is mostly micro-structural in the initial stage which with time reduces the life of the ship. These ships are subjected to a lot of load and pressure which eventually leads to deterioration in the material. This deterioration may cause catastrophic failure of the structure leading to human and commercial loss. The accidents of "Erika" and "Prestige" [1] - [2] disturbed the Flora and Fauna of Brittany, Spain, and France. Fatigue failure has been one of the most significant causes of such incidents. For safeguarding these ships, "dry-docking" is the most common process for inspection. But this type of inspection is prone to human error and is costly. Such inspections also need the ships to be off-duty for days which can be economically non-profitable to commercial or military sectors [3]. So there has been a focus to carry out the research in doing a detailed study of the damage occurring in the ship steel experiencing continuous stress and strain. The continuous real-time structural health monitoring of the ship steel has become the priority to protect the ships from rupture by prematurely identifying the damage in it and has therefore become very challenging in the research area [3] - [4].To predict and locate fatigue cracks, non-destructive testing techniques such as Alternating Current Field Measurement (ACFM) [5], Ultrasonic Testing (UT) [6], and Electromagnetic Acoustic Transducer (EMAT) [7] have been used. These are offline testing methods. This study aims to predict fatigue cracks in real-time and avoid future disasters. A recent study proposed a math-physic model of skewness to quantitatively characterise crack depth in a rail sample using eddy current pulsed thermography (ECPT) for depth estimation of rolling contact fatigue crack [8]. ECPT has proven to be effective in material characterization and nondestructive testing [8]. Though this method is effective for detecting defects in conducting materials, it falls short of proactively detecting defects.

The acoustic emission (AE) method is a very popular method for real-time non-destructive inspection of these structures and has turned out to be very efficient to monitor and analyse damage occurring in different materials [4], [9]-[10]. Acoustic emission is a nondestructive testing (NDT)

Prasannata Bhange, Deepak Kumar Joshi, Sunil Kumar Pandu, Kamal Mankari and Amit Acharyya are with Department of Electrical Engineering, Indian Institute of Engineering Hyderabad, Telangana-502285, India. (email: ee20resch01003@iith.ac.in, ee19resch11011@iith.ac.in, pandu.sunilkumar@ee.iith.ac.in, kamal.mankari@ee.iith.ac.in and and amit_acharyya@ee.iith.ac.in)

Swati Ghosh Acharyya is with School of Engineering Sciences and Technology, University of Hyderabad, Gachibowli, Telangana-500046, India. (email: sgase@uohyd.ac.in)

K. Sridhar is with Naval Materials Research Laboratory, Ambernath, Maharashtra-421506, India. (email: srid@nmrl.drdo.in)

This article has been accepted for publication in IEEE Sensors Journal. This is the author's version which has not been fully edited and content may change prior to final publication. Citation information: DOI 10.1109/JSEN.2022.3204146

technique that allows for the real-time prediction of fatigue crack growth in a material by implanting AE sensors on the ship structure, which continuously monitors it. In the primitive stages of research in the area of fatigue life prediction of composites, one of the research works was carried out on smooth tensile specimens and cracked fracture-toughness specimens. [11] showed that AE signals can be recorded whenever there is a plastic deformation [11] in such material. This study was restricted to loading the specimen in such a way that it does create noise and does not fall in the same frequency range as AE [11]. A de-noising method by [12] was developed based on translation invariant wavelet to eliminate noise from the AE signal. However, if the frequency of noise and crack information belong to the same frequency range then this method's efficacy would become questionable. Another work that focused on separating the peak and minimum load concluded that when a peak load is subjected to a specimen it results in crack extension, deformation, and fracture within the crack tip plastic zone [13], and when the minimum load is subjected to a specimen it indicates crack closure [13]. A relationship between crack growth rate and stress intensity factor during fatigue was given by [14] as $\frac{da}{dN} = C\triangle K^m$ where *a* represents crack length, *N* is the number of fatigue cycle, *K* is the stress intensity factor and *C* and *m* are assumed to be constants for a particular material [14]. Further AE count rate which is one of the AE parameters was related to the stress intensity factor and its relation was stated as $\frac{dn}{dN} = B\triangle K^p$ [15] where *n* is the count, *B* and *p* is assumed to be constants for a particular material [15]. It was found that there is a similar relationship between stress intensity factor and energy which was stated as $\frac{dU}{dN} = B_e\triangle K^p$ [16], where *U* is the energy and factor B_e is assumed to be constants for a particular material. This study of predicting crack growth is based on the material constant which will change with time and may predict the false crack growth values. A study on steel and welded steel compact tension (CT) specimens under fatigue showed a relationship between count rate and crack propagation [17]. The different acoustic emission (AE) parameters like rise time, the ratio of rise time to amplitude of the waveform (RA), and duration helped in estimating the crack propagation and could explain the transition from tensile to shear mode of the specimen after fatigue failure by visual analysis [18]. Above mentioned studies were related to threshold based AE parameters viz. rise time, duration, count, hit, load value, and number of cycle. In threshold-based studies, there is a chance of crack information loss. To overcome this a study on rail-track by using a technique called phase space reconstruction was done [19] to eliminate noise and detect crack was done. This study could suppress the noise to an extent and a model was built to distinguish abnormal noises and crack signals. An investigation on fatigue crack growth independent of the AE parameters was carried out by [20], which introduced a new parameter AE entropy. But as the load increases the prediction accuracy reduces.

In the view of above, it is apparent that a notable amount of research has been carried out to predict the damage occurrence in material under fatigue, however, it is also evident that there is still a need for a real-time method that could prematurely predict the crack propagation in such material. In this context, we presented recently our preliminary results in [21] by introducing briefly the concept of phase space reconstruction-based (PSR) crack growth rate prediction mechanism. However, in this article, we extend the concept presented in [21] by elaborating the PSR-based real-time prediction of crack growth rate, substantiating this methodology by experimental validation under various realistic fatigue scenarios that the ship undergoes, co-relating the results with micro-structural analysis using field emission scanning electron microscopy (FESEM) characterization. In this paper, a chaos-based phase space reconstruction methodology has been used to estimate the fatigue crack growth rate for structural health monitoring of ships. For this, three fatigue experimental setups were arranged where the DMR 249A ship steel was subjected to loading ratios of $R = 0.1, 0.25$, and 0.5. The AE sensors placed on top of these CT specimens could capture the AE waves radiated when these were subjected to a load. The pre-processing of the AE signals obtained from the AE sensor was done on the AE nodes connected to the AE sensors as shown in Fig.3.

The organization of the paper is as follows: Section II gives the details of the material used for the fatigue experiment and details about the fatigue experimental setup. Section III explains the proposed methodology. Section IV discusses the results of the proposed methodology and real-time estimation of the crack growth rate. The performance of the model has also been discussed in section IV.

II. Material and fatigue experimental details

In the current work, three fatigue experiments were carried out. The specimen used for the experiments was DMR 249A ship steel. Fig. 1a shows the FESEM micro-structure of the DMR 249A with the pearlite and ferrite phases. This specimen was prepared into a compact tension (CT) sample having a thickness of 10 ± 0.5 mm and width of 50 ± 0.10 mm. The specimen has been cut from DMR 249A plates keeping a chevron notch as per the ASTM E647 [22]. For linear crack propagation, the CT samples were pre-cracked for fatigue testing as shown in Fig.1b and is the CT specimen before the experiment started. Fig. 1c shows the CT specimen after the experiment. The fractograph of samples was characterized using a field emission scanning electron microscope for each R ratio (R = 0.1,0.25 and 0.5). Fig. 2 shows the striations produced in DMR 249 A for different R ratios and at different magnifications. Yellow arrows on the fractograph indicate the secondary cracks. Striations are the signature of fatigue failure. As the crack propagates and crack size increases the magnitude of stress concentration at the crack tip increases resulting in a) increase in stress intensity factor and b) an increase in the size of the plastic zone ahead of the crack tip. During the tensile half of the fatigue cycle, the crack propagates and crack closure occurs during the compressive cycle. A striation is formed when a crack blunts and stops propagating. Hence striations are found on the fracture surface of fatigue failure throughout the path of crack propagation [23] - [25].

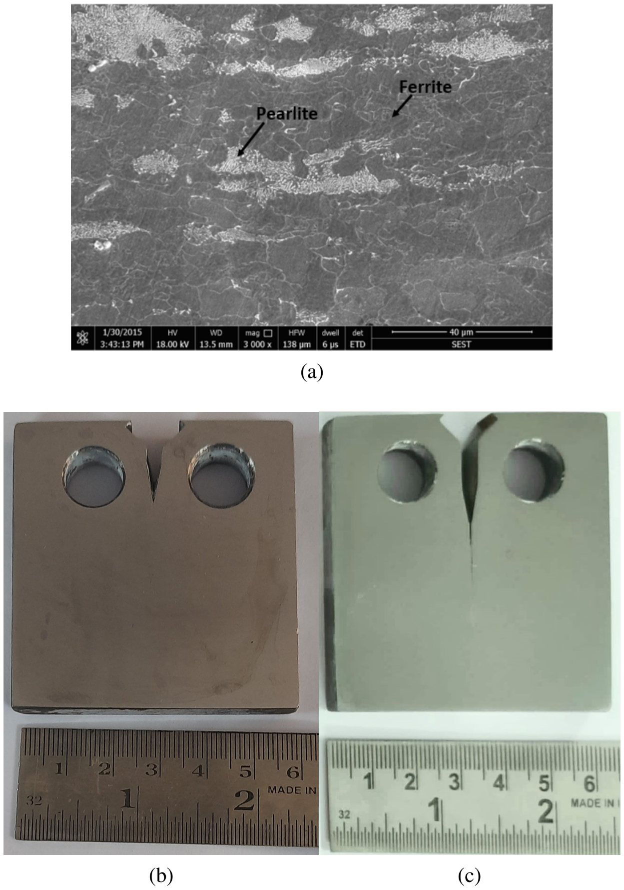

Fig. 1: a) Micro-structure of the CT specimen (Magnification = 3000 x), b) CT specimen before and c) CT specimen after experiment

The dislocation pile-up occurring at different locations such as the plastic zone and near the free surface of the crack result in the generation of a high magnitude of localized residual stresses. When the residual stresses exceed the critical value cracks initiate at different locations. An experimental setup for fatigue has been arranged to capture and analyse the AE signals as shown in Fig. 3. The sensors were placed on the CT samples with the help of adhesive tape and couplant. The sensors were connected to the AE node by Physical Acoustics Ltd for the pre-processing of signals which were connected to the AE software on a PC or laptop to capture the signals. The sampling rate of 5 MHz was chosen with a sample length of 7168. A 25 kN fatigue mechanical machine by Biss [27] was used for providing fatigue loading to the CT samples with the loading ratios of $(R = P_{min}/P_{max})$ 0.1, 0.25, and 0.5 which are mostly experienced in the real sea conditions with the sea-state value 4. Minimum and maximum load are represented by P_{min} and P_{max} respectively. CT sample dimensions were measured with the help of vernier calipers. The AE sensors used during the experiments were the wideband sensors by Physical Acoustics Ltd with the frequency ranging from 100 KHz to 1MHz as shown in Fig. 3.

III. Proposed Methodology

In this paper, a real-time fatigue crack growth rate estimation methodology has been developed for structural health

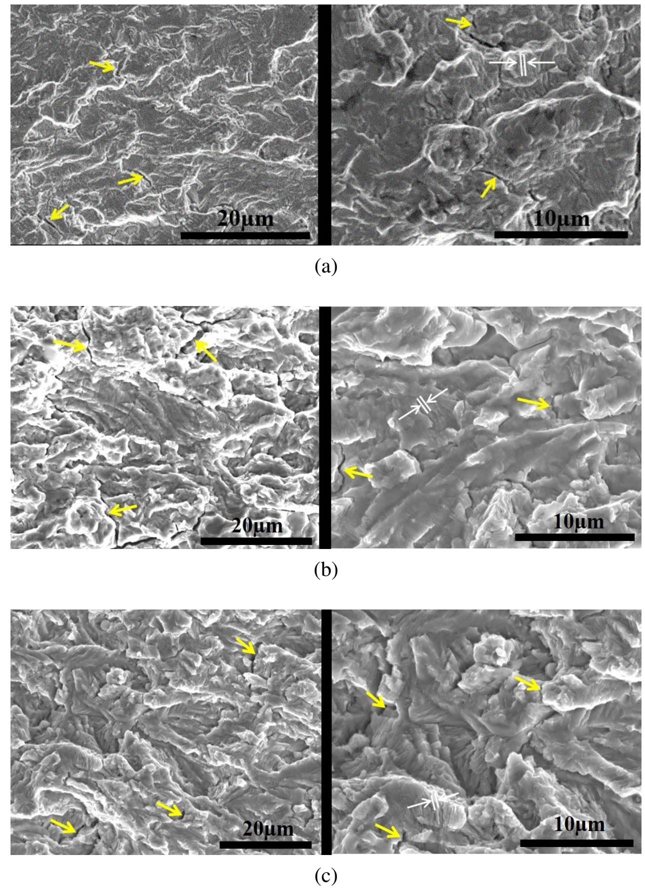

Fig. 2: FESEM micrographs of DMR 249A (magnification: 5000x and 10000x) a) R=0.1, b) R=0.25, and c) R=0.5 (yellow arrows indicate secondary cracks and white arrows indicate striations)

monitoring of ships where phase space reconstruction (PSR) technique has proved to be highly beneficial to identify even a small de-synchronization in a signal. The PSR technique for chaotic time series analysis has been introduced as the signals acquired through the AE sensors while the CT specimen was undergoing deterioration in the material are chaotic and non-stationary in nature [28]. Therefore, for predicting the damage in the material PSR technique has been introduced in this context.

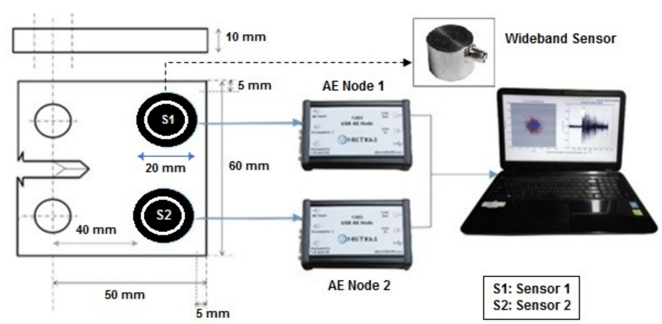

Fig. 3: Schematic of CT sample and location of wide band AE sensors (S1 and S2)

In this technique phase portraits are created by plotting the original AE signal with respect to its delayed signal. Consider a time series, $x(t) = x_1, x_2, x_3, ..., x_n$ and delay of τ then $x(t+\tau) = x_{1+\tau}, x_{2+\tau}, x_{3+\tau}, ..., x_{n+\tau}$. When $x(t)$ and $x(t+\tau)$ are plotted with respect to each other they form a phase portrait. The number of samples received from the sensors are 7168 at a particular time instant and from now onwards will be referred as AE hit. So, one AE hits consists of 7168 samples. The delay value was selected statistically such that the phase space trajectories form a pattern. One phase portrait is constructed from a trajectory of 7168 co-ordinate points. In Fig. 4a as an illustration the signals within the red boxes (box starting from 1 to 7168 samples and second box starting from 21 to 7188 samples) are plotted against each other to obtain one phase portrait. Similarly, to form the next phase portrait(Fig. 4b) the samples within the first red box is slided by τ (as an e.g. let us consider τ = 20 samples) to get the first green box (i.e. box starting from 21 to 7188 samples) and in the same way the second red box is slided by τ = 20 samples (i.e. box starting from 41 to 7208 samples) which are within the second green box are plotted against each other. The Fig. 4b indicates the phase portrait for time domain signal shown in Fig. 4a.

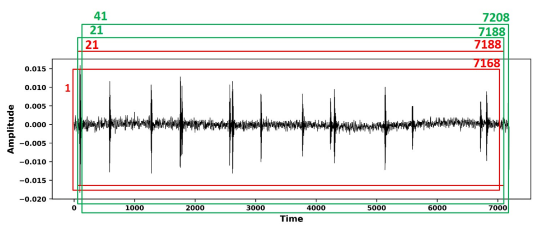

(a)

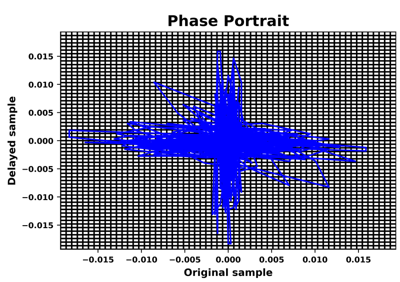

(b)

Fig. 4: (a) Time domain signal obtained from the in-situ AE sensors while doing the experiment on the ship's steel. (b) Phase portrait formed after applying the proposed phase space reconstruction technique on Fig.4a (for e.g. as an illustration the red and green boxes in Fig.4b are plotted against each other to obtain phase portrait.)

Monte-Carlo simulations were done to choose the delay value. The simulations were done on 10 different delay values for τ = 1, 2, 3, 4, 5, 10, 20, 25, 30, 35. Based on this simulation, we could visualise a pattern for a pure noise signal which was acquired during the experiment at the delay value of 20. Fig.5 shows the phase portraits with 10 different delay values with its corresponding time domain signal. The AE signal captured during the fatigue experiment consists of noise as well as crack information. To examine these signals the noise signal was captured separately. The phase portraits were

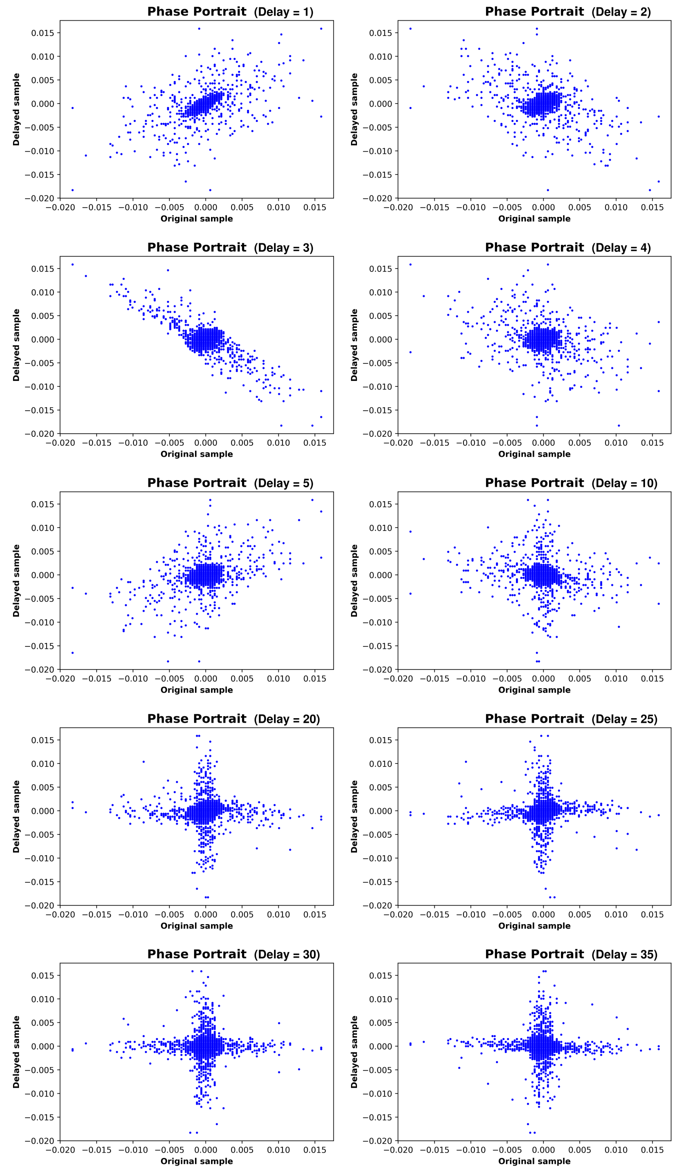

Fig. 5: Phase portraits of Monte-Carlo simulations done for delay i.e $\tau = 1, 2, 3, 4, 5, 10, 20, 25, 30, 35$ respectively.

created for noise signal and mixed signal (noise and crack information). The Fig. 6a is a hypothetical figure with a zero line in the absence of any noise and signal which is produced here for ease of understanding and explanation purposes. The respective phase portrait is also shown beside the time domain signal which shows there is no phase as such as per the expectations. Then the Fig. 6b shows a zero line followed by noise and the respective phase portrait is also drawn adjacent to it. It can be observed that it is more chaotic than Fig. 6a and it is also reflected in the value of the box count. In a similar way Fig. 6c provides the noise signal throughout the window and the respective phase portrait is more chaotic and is getting reflected in the box counts. In Fig. 6d we have the crack information signal coming in after the noise signal which is also validated by the fatigue machine and was time matched, which proves that the burst of the signal coming is due to the crack propagation. The number of box counts is also increased signifying that more chaos is introduced into the system. Fig. 6e also emphasizes when the burst of the crack, signal as well as the noise signal, is present in the time domain signal, the phase portrait is even more chaotic which is reflected in the number of box count which is 750, and is significantly more as compared to Fig. 6a to Fig. 6d. As a result, the manifestation of the noise and crack signal has been prominent in the phase portraits and can be seen clearly throughout Fig. 6. These observations aided in comprehending and differentiating the noise and crack information. These observations were evident for all the different loading ratios on testing (R=0.1, 0.25, and 0.5). The above observations helped in identifying the noise and crack information by providing the time domain signal as the input. Equal-sized 60×60 grids were created on the phase portraits after doing the Monte-Carlo analysis on various $(n \times n)$ grid sizes and it was observed $n = 60$ results in segregating the noise and crack in a optimum fashion for our proposed methodology. All the 3600 grids (60×60) were assigned box or grid numbers serially. As per the observations seen in Fig. 6 the noise signal points will fall in particular boxes where the pattern is formed and when the crack propagates the signal points will fall around the pattern. In this way, the specific boxes were assigned to the category of noise and the crack information as shown in Fig. 7 along with the zoomed-in version of the regions. If the co-ordinates fall inside the particular boxes which were assigned to noise only (blue scattered points) then the signal consists of only noise information. If the co-ordinates fall inside the particular boxes which were assigned other than that of noise that is around the pattern then the signal consists of crack information (red scattered points). The noise information was indicated by blue scattered points in the phase portrait and the crack information was indicated by red scattered points in the phase portrait. This methodology was applied to all the loading ratios i.e. 0.1, 0.25, and 0.5 and it worked efficiently on all. The phase portrait's axis value was made flexible in accordance with the amplitude value. Algorithm 1 shows the pseudo code for detecting cracks in the AE signal. The number of boxes occupied by the co-ordinate points of the phase space trajectories was counted by the technique called box-counting. The phase space trajectory formed by the co-ordinate points $(x_{original}, x_{delayed})$ falling on the boxes was examined by a very well-known technique called box-counting [29]. The spread of the trajectory was analyzed by counting the number of boxes occupied by the scattered points. In one of our previous research [29] work carried out in our laboratory for monitoring the cardiovascular well-being of a patient, it was observed that when a disease creeps into a healthy subject the cardiovascular system of that particular subject would become chaotic which can be measured using the box count after applying the phase space reconstruction technique. So drawing an analogy between the cardiovascular health of a living subject with a non-living structure under a different fatigue load where the crack has been propagated also would be chaotic in presence of a crack which perhaps can be assessed doing a phase space reconstruction using the box count methodology. With this hypothesis, we began our

Algorithm 1: Pseudo code

Step 1: $x_{original} : x_1, x_2, \cdots, x_n$
// $x_{original}$ is the data obtained from the AE sensor. Delay = τ, Sliding window = 20
$x_{delayed} : x_{1+\tau}, x_{2+\tau}, \cdots, x_{n+\tau}$
// $x_{delayed}$ is the delayed value of $x_{original}$.
Step 2: Axis calculation for phase portraits:
$x_{max} = max(x_1, x_2, \cdots x_{n+\tau})$;
$x_{min} = min(x_1, x_2, \cdots x_{n+\tau})$;
$abs_{max} = absolute(x_{max})$;
$abs_{min} = absolute(x_{min})$;
$a = max(abs_{max}, abs_{min}), axis\_value = a + 0.001$;
$axis\_final = -axis\_value$ to $+axis\_value$;
Step 3: Grid size = 60×60;
// The grid size is set to 60× 60 so that the grids can be plotted (fig. 6a) according to the axis calculated in **Step 2** for the box counting technique which will be used in the subsequent steps.
Step 4: Drawing grid lines: For drawing the grid lines, calculation of the co-ordinates where the lines are plotted are given as follows,
Co-ordinates for vertical grid lines = $vert\_sample$:
$(-a, -a + \frac{a}{60}, -a + \frac{a}{60} + \frac{a}{60}, \cdots, +a)$
Co-ordinates for horizontal grid lines = $hort\_sample$:
$(-a, -a + \frac{a}{60}, -a + \frac{a}{60} + \frac{a}{60}, \cdots, +a)$
Step 5: x_{id1} and y_{id1} are the arrays where its value is "1" if the $x_{original}$ and $x_{delayed}$ are greater than $vert\_sample$ and $hort\_sample$ respectively.
if $x_{original} >= vert\_sample$: **then**
    $x_{id1} = 1$;
else
    $x_{id1} = 0$;
end
if $x_{delayed} >= hort\_sample$: **then**
    $y_{id1} = 1$;
else
    $y_{id1} = 0$;
end
Step 6: Calculating the position of $x_{original}$ and $x_{delayed}$ in the grid
x_{id} = adding all the 1's in x_{id1}
y_{id} = adding all the 1's in y_{id1}
Step 7: Calculating the $cell_{id}$ for ($x_{original}$, $x_{delayed}$) co-ordinates : $cell_{id} = 60 \times (x_{id} - 1) + y_{id}$;
// $cell_{id}$ is an array which stores the box number of the co-ordinate $(x_{original}, x_{delayed})$.
Step 8: Saving the .csv file for box number and number of points falling in that box number.
Step 9: Array creation for different classification: Noise box array = (); **Step 10:**
if $cell_{id}$ = *Noise box array:* **then**
    scatterplot $(x_{original}, x_{delayed})$ in blue;
    //PSR technique
else
    scatterplot $(x_{original}, x_{delayed})$ in red;
    //PSR technique
end
Step 11: Calculating the mean of box count (*MBC*) for the one AE signal i.e. 7168 samples.
Step 12: Sliding the $x_{original}$ by sliding window (20 samples) and following the step one.

This article has been accepted for publication in IEEE Sensors Journal. This is the author's version which has not been fully edited and
content may change prior to final publication. Citation information: DOI 10.1109/JSEN.2022.3204146

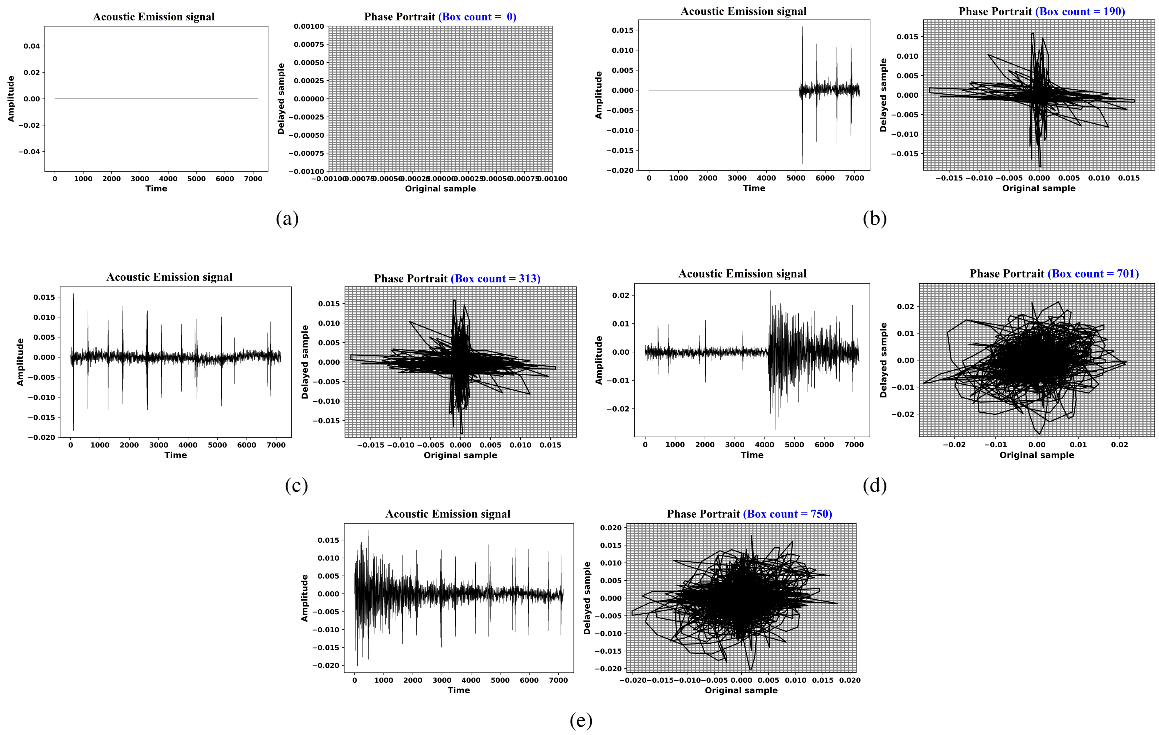

Fig. 6: Phase portraits of noise and mixed signal. a) Time domain and phase portrait for zero signal in the absence of any signal or noise, b) Time domain and phase portrait for zeros followed by noise signal c) Time domain and phase portrait noise signal d) Time domain and phase portrait for noise signal followed by mixed signal e) Time domain and phase portrait for mixed signal

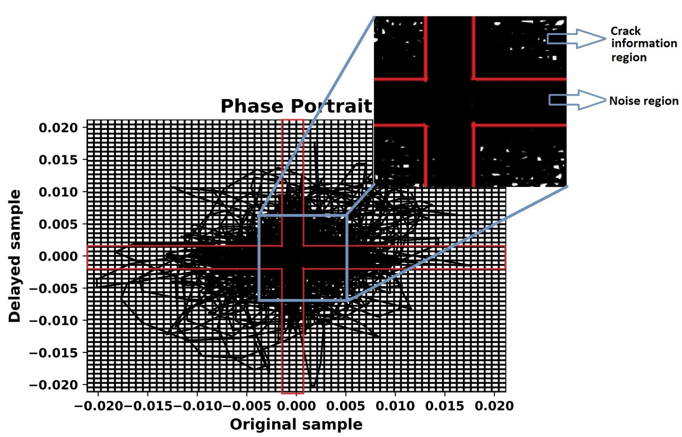

Fig. 7: Assigned region to noise and crack information

research work. After doing several tests under various fatigue loading our hypothesis was found to be true. The developed algorithm generates a numerical value known as box count, which is the number of boxes in the phase portrait occupied by the trajectory. When there is a delay of τ samples and a sliding window of k samples, N number of phase portraits for a signal of n samples are formed. Every N phase portrait has a box count value that is nearly the same. As a result, we calculated its mean in order to have a single mathematical parameter, namely the mean of box count (*MBC*) for an n-sample time domain signal. For example, if τ is set to 20 and k is set to 20, the algorithm generates approximately N = 300 phase portraits for an n = 7168-sample signal. Each phase portrait has a box count value that is nearly identical across all N = 300 phase portraits. As a result, it's mean has been computed for a single mathematical parameter, namely *MBC*. In contrast to when a noise signal is captured, *MBC* values increase as the crack grows, which correlates with the crack growth rate. The crack growth rate value is predicted when the $norm(cumulative(log(MBC)))$ values are fed into the developed model. The development of the presented methodology for the prediction of the fatigue crack growth rate for structural health monitoring of ships which involves the introduction of time domain parameter *MBC* using the phase space reconstruction technique in itself is a novel approach of the research work. The *MBC* values for the one time series signal are taken into consideration for the prediction of the crack growth rate. A polynomial regression-based model has been developed for predicting the crack growth rate. Polynomial regression analysis modelled a relationship between *MBC* and *CGR* as a 6th-degree polynomial. The *MBC* for a complete time series signal has been used in the polynomial regression model. Polynomial regression model is explained below:
Consider,

$$MBC = \{MBC_i\}, i \in (1, n). \tag{1}$$

where, i is the number of AE hit obtained from the AE sensor at a particular time instant while the specimen was under the fatigue loading. n = total number of AE hits obtained for each experiment (e.g. MBC_1 imples the mean of box count obtained at AE hit $i = 1$)

Now representing,

$$log(MBC_i) = m_i, i \in (1, n), \tag{2}$$

(For eg. MBC_i for $i = 1$ means Mean of Box Count computed for the first AE hit.) Cumulative of Eq.(2) can be computed as:

$$cum_j = \begin{cases} m_j, & j = 1 \\ cum_{j-1} + m_j, & 1 < j \leq n \end{cases} \tag{3}$$

Now introducing another term x_i which can be represented using Eq.(3) as follows,

$$x_i = \frac{cum(m_i) - min[cum_j]}{max[cum_j] - min[cum_j]}, (i, j) \in (1, n). \tag{4}$$

$min[cum_j]$ and $max[cum_j]$ are the minimum values and maximum values of cum_j respectively where $j \in (1, n)$. The crack growth rate (*CGR*) obtained from the fatigue machine log during the experiments can be represented as follows,

$$y_i = \frac{da}{dN}, \tag{5}$$

where, a = crack length and N = cycle. y_i represents CGR which is logged during the fatigue experiments. But it can be noted that y_i cannot be measured in the real-time and hence it has to be estimated using x_i which can be computed in real-time from the AE sensors. Hence, the next step of our proposed methodology is the fitting optimally the x_i onto y_i considering the fitted signal will be y'_i and it can be represented as follows,

$$y'_i = \beta_k(x_i^k) + \beta_{k-1}(x_i^{k-1}) + \cdots + \beta_0. \tag{6}$$

The next step is to find the value of k. Considering the fatigue log data i.e. y_i obtained fatigue machine, computed x_i value from the AE signals received from the AE sensors and various values of k after doing Monte-Carlo simulations it has been found that optimum value for k is 6. Hence, Eq.(6) can be re-written as,

$$\begin{aligned} y'_i = \beta_6(x_i^6) + \beta_5(x_i^5) + \beta_4(x_i^4) + \beta_3(x_i^3) + \beta_2(x_i^2) \\ + \beta_1(x_i^1) + \beta_0. \end{aligned} \tag{7}$$

$\beta_0, \beta_1, \beta_2, \beta_3, \beta_4, \beta_5$ and β_6 are the model parameters. It was observed that $y'_i \approx y_i$. This efficacy of the proposed methodology will be demonstrated in the next section.

IV. Result and Discussion

The proposed methodology identifies noise and cracks propagation in the given time-domain input signal obtained from the AE sensors. This methodology can be used in real-time crack monitoring by just creating the phase portraits of the time domain signal. In Fig. 8a time domain input signal captured is noise and its phase portrait is shown in Fig. 8b where the blue scattered points indicate noise in the input signal. In Fig. 8d, the phase portrait indicates crack propagation as red scattered points appear along with the presence of noise as blue scattered points also appear in the phase portrait.

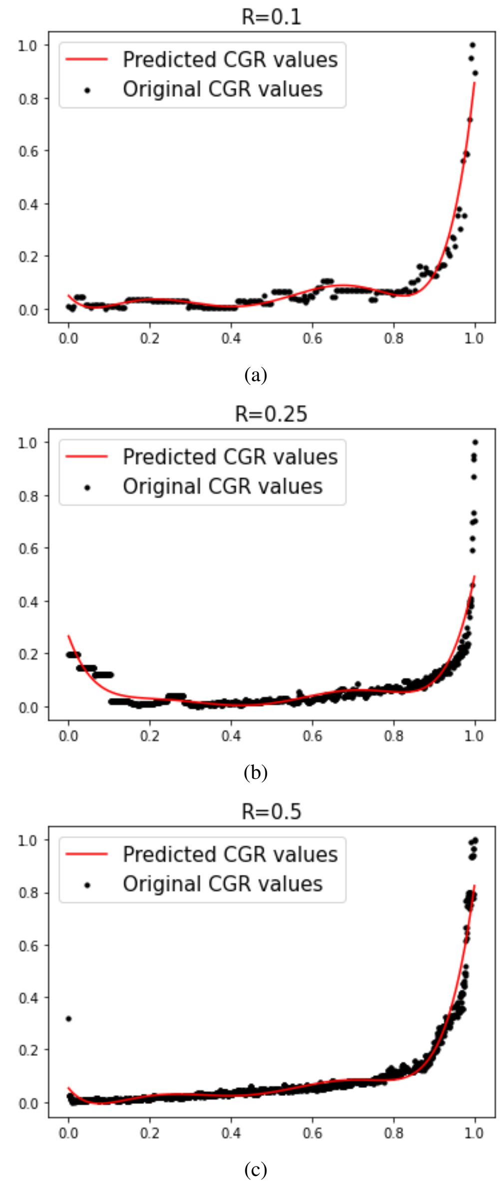

Fig. 9: Predicted CGR values. a) R=0.1, b) R=0.25 and c) R=0.5

Fig. 8c shows the corresponding time domain signal of Fig. 8d. Fig. 8f shows another phase portrait of a mixed signal as shown in Fig. 8e indicating crack propagation in the material as the red scattered points appear in the phase portrait. Similarly, for the time domain signal in Fig. 8h the phase portrait generated is as shown in Fig. 8g and indicates crack propagation in the material as red scattered points appear along with the noise signal. The crack growth rate log obtained during the experiment from the fatigue machine was used to validate the crack information produced by the model. This methodology is independent of the parameters like counts, energy, time of the event, rise time, duration, etc. The polynomial regression model of sixth-degree order creates a best-fit line for *CGR* as shown in Fig. 9. The RMSE and R-

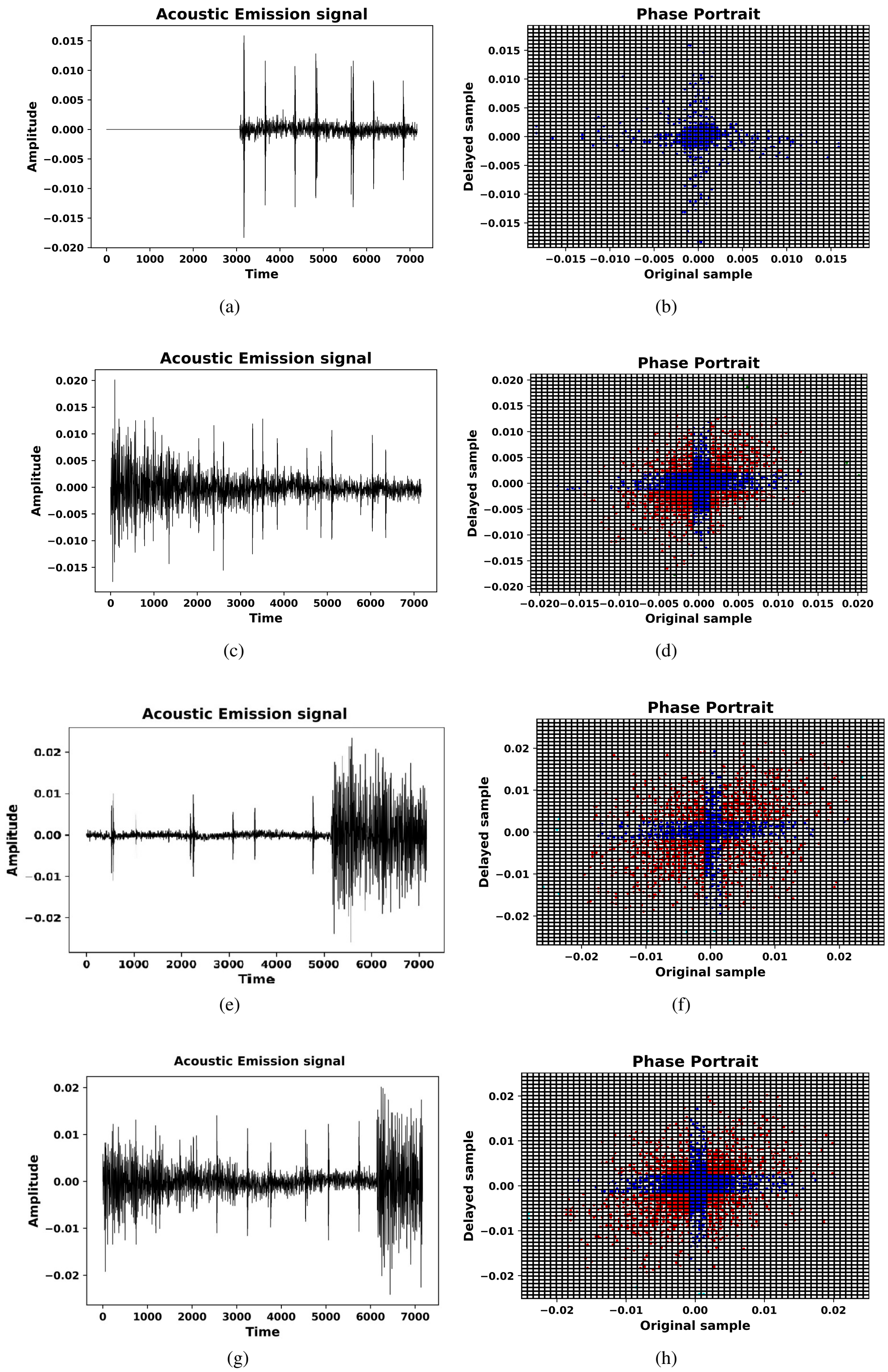

Fig. 8: Phase portrait of noise and different mixed signal. a) time domain for noise signal, b) Phase portrait for noise signal. c), e) and g) are the different time domain mixed signals. d), f) and h) are the phase portraits respectively.

squared values of the model show good performance as shown in Table I.

TABLE I: Root Mean Square Error and R-squared values of the model

Loading Ratios	R=0.1	R=0.25	R=0.5
RMSE	0.03	0.03	0.028
R^2 (co-efficient of determination)	0.93	0.80	0.95

Hence it can be concluded that the current methodology predicts the fatigue crack while it is growing, in contrast to the existing approaches (ACFM, UT, EMAT, etc.), which inspect the crack after it has already grown. The advantages of the methodology presented in this work forecast a fatigue crack growth rate in real-time utilising a time domain signal recorded by acoustic emission sensors installed on the structure. Secondly, the proposed phase space reconstruction method makes it possible to understand the significantly small change in a time domain signal, which helps in capturing every crack propagation information in a real-time signal. Furthermore, the proposed methodology does not take into consideration the classical threshold-based parameters, including AE count, AE count rate, duration, etc., and therefore it is not limited by a fixed threshold value. However, the proposed methodology is validated against the laboratory-based experiments and as part of our future research, in order to translate this methodology to a viable practical solution, rigorous testing needs to be done after the on-field deployment.

V. Conclusion

The first of its kind estimation of fatigue crack growth rate propagation using PSR-based technique for a DMR 249A ship steel specimen for the application of structural health monitoring of ships has been done in this paper. The CT specimen prepared from this ship steel was loaded with real sea state conditions having a sea state value of 4 by the fatigue loading machine. The loading ratios for the experiments were $R = 0.1, 0.25$ and 0.5. AE sensors being placed on the CT specimen were able to capture the time domain signal, which was then pre-processed by the physical acoustic node. AE signals were captured for any dislocations occurring in the material. A methodology based on the PSR technique was developed to identify the crack occurring in the material. This methodology has proven to be capable enough to identify the noise and crack information from the phase portraits created. A new parameter *MBC* was introduced and was beneficial in estimating the crack growth rate using the polynomial regression-based model.

Acknowledgment

We acknowledge the funding received from the Naval Research Board, India, and the Department of Science and Technology SERB IMPRINT for carrying out this study. We sincerely thank Jalaj Kumar from Defense Materials Research Laboratory, Kanchanbagh, Hyderabad, Telangana and Giri R. Gunnu from Tardid Technologies Pvt. Ltd. Bengaluru, Karnataka for providing their inputs from time to time.

References

[1] French Marine Accident Investigation Office (BEAmer). Report of the enquiry into the sinking of Erika Off the Coast of Brittany on 12 December 1999.
[2] American Bureau if Shipping, Technical Analysis Related to the Prestige Casualty on 13 November 2002.
[3] Miroyannis, A.,"Estimation of Ship Construction Costs", (B.S. thesis). Department of Mechanical Engineering, Massachusetts Institute of Technology, Boston, MA,2006.
[4] Vassilios Kappatos, Evangelos Dermatas, "Structural health monitoring of ship and other offshore structures using acoustic emission testing", Justin K. Burnett, editors, *Theory and Uses of Acoustic Emissions*, chapter 5, pages 95-106, Nova Science Publishers 2012.
[5] Zhou L, Brunskill H and Lewis R., "Non-invasive measurement and monitoring of wheel-rail contact using ultrasonic reflectometry", Struct Health Monit, 18(5–6):1953–1965
[6] Rowshandel, Hamed, et al. "Characterisation of clustered cracks using an ACFM sensor and application of an artificial neural network.", NDT and E International 98, 2018 : 80-88.
[7] Thring, C. B., Y. Fan, and R. S. Edwards.,"Multi-coil focused EMAT for characterisation of surface-breaking defects of arbitrary orientation.", NDT and E International 88, 2017: 1-7.
[8] Liu, Yi, et al. "Depth quantification of rolling contact fatigue crack using skewness of eddy current pulsed thermography in stationary and scanning modes.", NDT and E International 128, 2022 : 102630.
[9] C. Xu, S. Du, P. Gong, Z. Li, G. Chen and G. Song, "An Improved Method for Pipeline Leakage Localization With a Single Sensor Based on Modal Acoustic Emission and Empirical Mode Decomposition With Hilbert Transform.", in IEEE Sensors Journal, vol. 20, no. 10, pp. 5480-5491, 15 May15, 2020, doi: 10.1109/JSEN, 2020, 2971854.
[10] Y. Zhang, Z. Wen, B. Li and H. Wu, "Experimental research on acoustic emission characteristics in damage process of different meso-structural specimens,." 2015 Symposium on Piezoelectricity, Acoustic Waves, and Device Applications (SPAWDA), 2015, pp. 467-470, doi: 10.1109/SPAWDA.2015.7364532.
[11] H. Dunegan and D. Harris,"Acoustic emission-a new non-destructive testing tool", Ultrasonic July, 1969.
[12] Jiang Changhong, Wang Longshan, Yon Wen and Liu Zhixin, "Research on acoustic emission signals de-noising based on translation invariant wavelet", 30th Annual Conference of IEEE Industrial Electronics Society, 2004. IECON 2004, 2004, pp. 1775-1778 Vol. 2, doi: 10.1109/IECON.2004.1431851.
[13] T. C. Lindley, I. G. Palmer* and C. E. Richards, "Acoustic Emission Monitoring of Fatigue Crack Growth", Material Science and Engineering, 32, 1 – 15, 1978.
[14] Paris, P. C.; Erdogan, F., "A critical analysis of crack propagation laws", Journal of Basic Engineering, 1963.
[15] Maddox SJ., "Fatigue strength of welded structures", Cambridge: Abington Publishing, 1991.
[16] Y.Jianguo, P.Ziehl, B. Zarate, J.Caicedo., "Prediction of fatigue crack growth in steel bridge components using acoustic emission", Journal of Constructional Steel Research 2011; 67: 1254-1260.
[17] Z Gong, EO Nyborg, G Oommen., "Acoustic emission monitoring of steel railroad bridges", Materials Evaluation, 1992; 883-887.
[18] Aggelis, D., Kordatos, E. and Matikas, T., "Acoustic emission for fatigue damage characterization in metal plates", Mech. Res. Commun., 38(2), 2011, 106-110.
[19] Xin Zhang , Qiushi Hao , Kangwei Wang , Yan Wang , Yi Shen ,Hengshan Hu, "An investigation on acoustic emission detection of rail crack in actual application by chaos theory with improved feature detection method", Journal of Sound and Vibration 436; 2018, 165-182.
[20] Mengyu Chai, Zaoxiao Zhang, Quan Duan, Yan Song , "Assessment of fatigue crack growth in 316LN stainless steel based on acoustic emission entropy", International Journal of Fatigue, 2018.
[21] Prasannata Bhange, Deepak Kumar Joshi, P Sunil Kumar, Kamal Mankari, Swati Ghosh Acharyya, K Sridhar and A. Acharyya, "Phase Space Reconstruction Based Real Time Fatigue Crack Growth Estimation for Structural Health Monitoring Ships", 2022 IEEE Latin American Symposium of Circuits and Systems (LASCAS), Chile, 2022.
[22] American Society for Testing and Materials (ASTM), "ASTM E647: standard test method for measurement of fatigue crack growth rates", in Annual Book of ASTM Standards, vol. 03.01, pp.
[23] Laird, C. "The Influence of Metallurgical Structure on the Mechanisms of Fatigue Crack Propagation."; ASTM International: West Conshohocken, PA, USA, 1967; p. 36.

[24] Gauthier, P.; De Rabaudy, H.; Auvinet, J. "Secondary cracking process during fatigue crack propagation."; Eng. Fract. Mech. 1973, 5,977–981.

[25] Bai, J.-B.; Chen, S.-Y. "Secondary cracking during surface crack growth under tensile fatigue loading."; Eng. Fract. Mech. 1988, 30,161–167.

[26] Zhu, Q.; Zhang, P.; Peng, X.; Yan, L.; Li, G. "Fatigue Crack Growth Behavior and Fracture Toughness of EH36 TMCP Steel."; Materials 2021, 14, 6621. https://doi.org/10.3390/ma14216621

[27] BISS : Nano Plug and Play, 2020. Accessed on: September. 15, 2021.

[28] R. J. Povinelli, M. T. Johnson, A. C. Lindgren, F. M. Roberts and Jinjin Ye, "Statistical models of reconstructed phase spaces for signal classification," in IEEE Transactions on Signal Processing, vol. 54, no. 6, pp. 2178-2186, June 2006, doi: 10.1109/TSP.2006.873479.

[29] Naresh Vemishetty, Ramya Lakshmi Gunukula, Amit Acharyya, Paolo Emilio Puddu, Saptarshi Das and Koushik Maharatna, "Phase Space Reconstruction Based CVD Classifier Using Localized Features", Scientific Reports, 2019.

Prasannata Bhange received the B.Tech. and M.Tech. degrees from Nagpur University, Maharashtra, India, in 2016 and 2019, respectively, and she is currently pursuing the Ph.D. degree in micro-electronics and VLSI with the Department of Electrical Engineering, Indian Institute of Technology Hyderabad, Hyderabad, India. Her research interests include signal processing algorithms and deep learning for structural health monitoring.

Deepak Kumar Joshi received the B.Tech. degree from Rajiv Gandhi Technical University, Madhya Pradesh, India, in 2016 and M.Tech. degree from Devi Ahilya University in 2019. He is currently pursuing the Ph.D. degree in microelectronics and VLSI with the Department of Electrical Engineering, Indian Institute of Technology Hyderabad, Hyderabad, India. His research interests include signal processing, signal analysis and deep learning algorithms for structural health monitoring.

Sunil Kumar Pandu received the B.Tech. degree from D V R College of Engineering and Technology, Jawaharlal Nehru Technological University, Andra Pradesh, India, in the field of Mechanical Engineering in 2009 , M.E. degree from Osmania University, Andra Pradesh, India in 2012 and the Ph.D. degree from University of Hyderabad, Hyderabad, India in the field of Materials Engineering in 2021. His research interests include studying the mechanical behaviour of materials, manufacturing technology, corrosion engineering, surface engineering, and physical metallurgy.
Dr. Pandu is currently working as research fellow with the Indian Institute of Technology (IIT) Hyderabad, Hyderabad, India.

Kamal Mankari received the B.Tech. degree from Mahatma Gandhi Institute of Technology, Hyderabad, India, in the field of Metallurgy and Materials Engineering in 2010 , M.Tech. degree from University of Hyderabad, India in the field of Materials Engineering in 2013 and the Ph.D. degree from University of Hyderabad, Hyderabad, India, in the field of Materials Engineering in 2019. His research interests include studying the mechanical behaviour of materials, manufacturing technology, corrosion engineering, surface engineering, and physical metallurgy.
Dr. Mankari is currently working as research fellow with the Indian Institute of Technology (IIT) Hyderabad, Hyderabad, India.

Swati Ghosh Acharyya received the B.E. degree from National Institute of Technology, Durgapur, India, in the field of Metallurgical Engineering in 2005 , M.Tech. degree from Indian Institute of Technology Kharagpur, Khragpur, India in the field of Metallurgical and Materials Engineering in 2007 and the Ph.D. degree from Homi Bhabha National Institute (DAE) India, in the field of Materials Engineering in 2012. Her research interests include materials research especially on corrosion of different alloys used for fabrication of structural components in nuclear power plants.
She worked as a Scientific Officer in Corrosion Science Section, Materials Science Division, Bhabha Atomic Research Centre (BARC), Mumbai, India from 2007 to 2013.
Dr. S.G. Acharyya is currently working as Associate Professor with the University of Hyderabad, Hyderabad, India.

K. Sridhar received the PhD degree from Indian Institute of Technology Bombay in 1998. He has done his postdoctoral work at Boston University, USA in PVD coatings.
He is working as senior scientist at Naval Materials Research Laboratory of Defence Research and Development Organisation (DRDO) in the field of Surface engineering for localized corrosion and erosion-corrosion resistance using Fe-based amorphous powders, fatigue, Corrosion fatigue and stress corrosion cracking studies on ship building steels, welds and residual stress measurement of welds since last 30 years. He has published around 50 papers including 4 chapters in ASM handbooks and Encyclopedia of steels and alloys. He is a reviewer for five international journals. He was awarded best Ph.D thesis by NACE international (1998) for his thesis work at IIT Bombay and Laboratory scientist of the year (2017).
Dr. K. Sridhar is currently working as senior scientist at Naval Materials Research Laboratory of DRDO.

Amit Acharyya received the Ph.D. degree from the School of Electronics and Computer Science, University of Southampton, U.K., in 2011. He has authored more than 80 international refereed journals and more than 90 international peer reviewed conferences and contributed towards 6 book chapters. His research interests are in the area of VLSI systems for resource-constrained applications, low power design techniques, machine learning hardware design, edge computing, healthcare technology and chip-design targeting remote health monitoring including cardiovascular diseases, diabetes, autism spectrum disorder, neurological disorder, orthopedically handicapped patients, accelerating cancer diagnostic procedures through hardware software co-design, signal processing algorithm and VLSI Architectures, digital arithmetic, and hardware security. He is also handling several projects of Government of India including Science and Engineering Board (SERB), Department of Science and Technology (DST), Ministry of Electronics and Information Technology (MEITY), and Defence Research and Development Organization (DRDO) apart from working in the private Industry sponsored projects including Xilinx, Inc., USA.
He worked as Scientist-B in Defence Research and Development Organisation from 2005 to 2007, Research fellow in University of Southampton U.K. in the year of 2011 and Assistant Professor (on contract position) in Indian Institute of Guwahati from 2011 to 2012.
Dr. Acharyya is currently an Associate Professor with the Indian Institute of Technology (IIT) Hyderabad, Hyderabad, India.